PHYSICAL REVIEW B 70, 121201(R) (2004)

Identification of Ga-interstitial defects in GaN_yP_{1-y} and $Al_xGa_{1-x}N_yP_{1-y}$

N. Q. Thinh, I. P. Vorona,* I. A. Buyanova, and W. M. Chen†
Department of Physics and Measurement Technology, Linköping University, 58183 Linköping, Sweden

Sukit Limpijumnong
School of Physics, Institute of Science, Suranaree University of Technology, Nakhon Ratchasima 30000, Thailand

S. B. Zhang
National Renewable Energy Laboratory, Golden, Colorado 80401, USA

Y. G. Hong and C. W. Tu
Department of Electrical and Computer Engineering, University of California, La Jolla, California 92093-0407, USA

A. Utsumi, Y. Furukawa, S. Moon, A. Wakahara, and H. Yonezu
Department of Electrical and Electronic Engineering, Toyohashi University of Technology, Toyohashi, Aichi 441-8580, Japan
(Received 29 June 2004; revised manuscript received 4 August 2004; published 13 September 2004)

Two Ga-interstitial (Ga_i) defects are identified by optically detected magnetic resonance as common grown-in defects in molecular beam epitaxial GaN_yP_{1-y} and $Al_xGa_{1-x}N_yP_{1-y}$. Characteristic hyperfine structure arising from spin interaction between an unpaired electron and a Ga nucleus is clearly resolved. The observed strong and nearly isotropic hyperfine interaction reveals an electron wave function of A_1 symmetry that is highly localized at the Ga_i and thus a deep-level defect. Our analysis based on first-principles calculations suggests that these defects are complexes containing one Ga_i^{2+}.

DOI: 10.1103/PhysRevB.70.121201 PACS number(s): 61.72.Ji, 61.72.Bb, 71.55.Eq, 76.70.Hb

Self-interstitials, together with vacancies and antisites, belong to an important class of defects, i.e., intrinsic defects, in compound semiconductors. They are commonly found in semiconductors grown under nonequilibrium conditions or subjected to high-energy particle bombardment, and could play a crucial role in the electronic and optical properties of semiconductors. Among a few successful experimental techniques, magnetic resonance techniques have been shown to be a powerful probe for investigating the chemical identity and microscopic structure of defects.[1–5]

Since the middle 1980s, optically detected magnetic resonance (ODMR) studies revealed that Ga self-interstitials (Ga_i) are common residual defects in bulk GaP (Refs. 6–8) and in epitaxially grown $Al_xGa_{1-x}As$ (Refs. 9 and 10), AlAs/GaAs superlattices,[11] and $GaAs/Al_xGa_{1-x}As$ heterostructures.[12] Recently, Ga_i has been shown to be among the dominant defects in epitaxial GaN films when they are exposed to high-energy electron irradiation after growth.[13,14] In one case, a complex involving a Ga_i was observed in as-grown Zn-doped GaN.[15] Though many models were proposed, the microscopic structures of Ga_i are still largely unknown.

In this work, we were able to identify two types of Ga_i defects (denoted below as Ga_i-*A* and Ga_i-*B*) by ODMR in the GaN_yP_{1-y} and $Al_xGa_{1-x}N_yP_{1-y}$ alloys. Both defects are shown to possess an electron wave function of A_1 symmetry that is rather highly localized at the Ga_i site. By taking advantage of the degree of freedom provided by this alloy system, the defects were investigated under varied compositions of both group-III and group-V atoms in the two sublattices.

The GaN_yP_{1-y} and $Al_xGa_{1-x}N_yP_{1-y}$ epilayers (with a thickness of 0.75–0.9 μm) studied in this work were grown on GaP substrates, by gas-source molecular beam epitaxy (MBE). Two sets of samples were used to investigate the effect of Al and N compositions on the defects. One set is $Al_xGa_{1-x}N_yP_{1-y}$ with a fixed N composition of $y=0.012$ but different Al compositions of $x=0$, 0.02, and 0.3. The other set is GaN_yP_{1-y} with varied N compositions ($y=0.012$, 0.023, 0.031). To examine if the defects under study are common in this class of alloy system, a 0.15-μm-thick $GaN_{0.018}P_{0.982}$ epilayer grown on a Si(100) substrate by solid-source MBE was also studied.

The ODMR measurements were performed at two microwave frequencies (~9.3 GHz and ~95 GHz). Photoluminescence (PL) was excited by the 532 nm line from a solid state laser and was detected by a cooled Ge detector and a GaAs photodiode for the near infrared and visible spectral range, respectively. ODMR signals were detected as spin-resonance-induced changes in PL intensity. The success of the ODMR technique in identifying the chemical nature of the Ga_i interstitials relies on its ability to measure the hyperfine (HF) interaction between an unpaired electron spin and the nuclear spin of the Ga_i, described by the spin Hamiltonian

$$H=\mu_B\mathbf{B}\cdot\mathbf{g}\cdot\mathbf{S}+\mathbf{S}\cdot\mathbf{A}\cdot\mathbf{I}. \quad (1)$$

Here the first and second terms describe electron Zeeman and HF interaction terms, respectively; μ_B is the Bohr magneton, $\mathbf{B}$ is the magnetic field; $\mathbf{g}$ is the Zeeman splitting tensor, and $\mathbf{A}$ is the HF interaction tensor for each of the two naturally abundant Ga isotopes (^{69}Ga and ^{71}Ga). The effective electron spin is $S=1/2$ and both Ga isotopes have the same nuclear spin of $I=3/2$. Both $\mathbf{g}$ and $\mathbf{A}$ tensors are de-

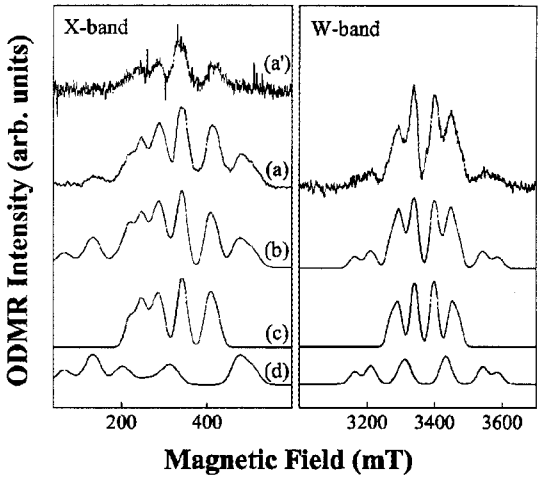

FIG. 1. (a) and (a′) Typical ODMR spectra from $Al_{0.02}Ga_{0.98}N_{0.012}P_{0.988}$ measured at 5 K and 40 K, respectively, at *X* band (9.31 GHz) and *W* band (94.8 GHz). The laser and microwave power used were about 2 and 200 mW, respectively. The microwave radiation was amplitude modulated at a frequency of 1.5–2 kHz and the resulting change of PL intensity (i.e., the ODMR signal) was detected by the lock-in technique. (b) The simulated ODMR spectra including the contributions from (c) the Ga_i-*A* defect and (d) the Ga_i-*B* defect with the spin Hamiltonian parameters given in Table I.

duced to be isotropic for both Ga_i-*A* and Ga_i-*B*, within the experimental accuracy, and are reduced to the scalars *g* and *A*.

For each microscopic configuration, the HF interaction tensor **A** can be calculated from the interaction between the spin density of the electron and the nuclear spins. Using state-of-the-art first-principles supercell calculations as implemented in the WIEN2k code,[16] we calculated the electron spin distribution topology that was then used to calculate the HF tensor. The calculations were based on generalized gradient approximations (GGA) within the framework of density functional theory (DFT), using all electron full-potential linearized augmented-plane-wave (FPLAPW) method. The relativistic effects were included through scalar relativistic treatment for valence electrons. Our test calculations of a well-established signature, Zn_i in ZnSe (Ref. 17), yielded the central HF parameter in good agreement with the experiment to within 10%. A supercell containing 32 atoms, which was sufficient to provide converged HF parameters,[18] was used. Electron density of a free atom was calculated by placing the atom in a large cubic supercell ($10\times10\times10$ Å) to reduce the intercell interactions.

Typical ODMR spectra from the studied $Al_xGa_{1-x}N_yP_{1-y}$ epilayers are shown in Fig. 1, where a single line with a *g* value close to 2 from a defect of unknown origin has been subtracted since it is not a subject of the present study. Except for a positive ODMR signal for $GaN_{0.018}P_{0.982}$ grown on Si by solid-source MBE, the ODMR signals have a negative sign, corresponding to a decrease upon spin resonance of PL intensities. Such a negative and emission insensitive ODMR signal indicates that these defects provide a shunt pass for carrier recombination competing with the PL (Refs. 4, 5, and 19). Temperature dependence studies reveal that the ODMR spectra are originated from two different defects (Ga_i-*A* and Ga_i-*B*), of which Ga_i-*B* loses signal strength at elevated temperatures and vanishes at $T>40$ K [see spectrum (a′) in Fig. 1].

The ODMR spectra at the *X* band are rather irregular, which makes it very difficult to assign them specific nuclear spin states. However, the ODMR spectra at the *W* band show a clear pattern with two groups of lines from Ga_i-*A* and Ga_i-*B* with distinct intensities. Each defect gives rise to two sets of four lines with a fixed intensity ratio of 40/60 and a fixed line spacing ratio of 1.3 (Fig. 1). The only plausible explanation is that each defect involves one Ga atom. This way, (i) the two Ga isotopes (^{69}Ga and ^{71}Ga) produce the two sets of four lines; (ii) the ratio of the natural abundance of the two isotopes, 39.6%(^{71}Ga)/60.4%(^{69}Ga), is consistent with the ratio of the ODMR intensity of 40/60; (iii) the ratio of the nuclear magnetic moments of the two isotopes, $\mu(^{71}\mathrm{Ga})/\mu(^{69}\mathrm{Ga})=1.27$, is consistent with the ratio of the ODMR line spacing of 1.3. Our ODMR results thus provide compelling evidence for the involvement of a Ga atom in the core of both Ga_i-*A* and Ga_i-*B* defects.

By fitting the spin Hamiltonian [Eq. (1)] to the experimental data, the spin Hamiltonian parameters were determined for both Ga_i-*A* and Ga_i-*B* in all samples (Table I). The quality of the fit can be seen, for e.g., in the simulated ODMR curves for $Al_{0.02}Ga_{0.98}N_{0.012}P_{0.988}$ at both microwave

TABLE I. Spin Hamiltonian parameters obtained by fitting Eq. (1) with the experimental data for Ga_i-*A* and Ga_i-*B* in GaN_yP_{1-y} and $Al_xGa_{1-x}N_yP_{1-y}$. Spin density η^2 at Ga_i is deduced from our calculated value of the charge density of the 4*s* electron. $A(^{71}\mathrm{Ga})$ can be determined by the relation $A(^{71}\mathrm{Ga})/A(^{69}\mathrm{Ga})=1.27$.

		Ga_i-*A*			Ga_i-*B*		
x	*y*	*g*	$A(^{69}\mathrm{Ga})(10^{-4}\ \mathrm{cm}^{-1})$	η^2 (Ga_i)	*g*	$A(^{69}\mathrm{Ga})(10^{-4}\ \mathrm{cm}^{-1})$	η^2 (Ga_i)
0	0.031	2.001	770	0.20	2.003	1150	0.30
0	0.023	2.001	770	0.20	2.003	1150	0.30
0	0.018		unresolved		2.003	1150	0.30
0	0.012		unresolved		2.005	1150	0.30
0.02	0.012	2.01	490	0.13	2.005	1030	0.27
0.3	0.012	2.01	450	0.12	2.005	980	0.25

frequencies in comparison with the measured spectra (Fig. 1).[20] The deduced isotropic g and A tensors, together with the rather strong HF interaction, point to the A_1 symmetry for the electron wave function localized at the Ga_i. For a free neutral Ga atom, we calculated the charge density of the 4*s* electron and found $|\psi_{4s}(0)|^2 = 72.7 \times 10^{24}$ cm^{-3}. This charge density corresponds to the ^{69}Ga HF interaction $A = 0.3855$ cm^{-1}. This is in good agreement with two prior calculations with relativistic effects included[21,22] i.e., (1) Hartree-Fock-Slater calculations by Morton and Preston[23] ($A = 0.4070$ cm^{-1}) and (2) DFT calculations by Van de Walle and Blöchl[18] ($A = 0.3277$ cm^{-1}). Based on our 4*s* charge density, we estimate the localization of the unpaired electron at the Ga_i to be in the range of 12–30 % (Table I). The rather strong localization indicates that these are deep-level defects.

To be a defect, a Ga atom can reside (1) on a site of the group-V sublattice forming a cation antisite or (2) on an interstitial position leading to a Ga self-interstitial. A Ga-related cation antisite in GaP has been predicted by earlier calculations[24] as well as our theoretical calculations to possess an electron wave function of T_2 symmetry, which will yield a very weak and anisotropic HF interaction at the defect center. This is clearly inconsistent with our experimental observation and therefore such an antisite can be ruled out. Our theoretical calculations also found the HF interaction of a neutral Ga_i to be weaker than 100×10^{-4} cm^{-1}, which is also inconsistent with our observed strong HF interaction. A Ga_i in the (2+)-charge state, on the other hand, is predicted to possess a strongly localized electron wave function of A_1 symmetry consistent with our measured results. Therefore we can conclude that the Ga atom in the Ga_i-*A* and Ga_i-*B* defects is indeed a Ga_i^{2+} interstitial.

Now the question is whether both Ga_i-*A* and Ga_i-*B* are just isolated Ga_i or they are Ga_i-related complexes. We believe the latter is true. Our calculations give much stronger HF interactions for isolated Ga_i in GaP, i.e., $A = 1876 \times 10^{-4}$ cm^{-1} for Ga_i at the T_d[Ga] site (the site surrounded by four Ga atoms) and $A = 1599 \times 10^{-4}$ cm^{-1} for Ga_i at the T_d[P] site. A reduced HF interaction is commonly regarded as evidence for complexing due to charge transfer or the redistribution of the electron wave function to neighboring atoms. We have calculated some of the Ga_i complexes and found large reductions of the HF interaction due to complex formation, as expected. Recent experimental ODMR studies for wurtzite GaN (Refs. 13 and 14) have convincingly shown that isolated Ga_i is unstable at temperatures well below room temperature and readily form complexes. Since the lattice constants of $Ga_{1-x}N_yP_{1-y}$ and $Al_xGa_{1-x}N_yP_{1-y}$ are considerably larger than that of GaN, Ga_i should migrate easier. Thus, the same conclusion should also hold here.

To provide more structural information on Ga_i-*A* and Ga_i-*B*, the chemical compositions of both group-III and -V sublattices were varied experimentally. The resulting HF interactions of the defects are summarized in Table I and Fig. 2. A rather strong reduction (about 10% for Ga_i-B) is observed even at a low Al composition (as low as 2%). With further increase in the Al composition, however, the rate of reduction is significantly reduced, i.e., by 5–8 % for the entire range of $x = 0.02$ to $x = 0.3$. This observation indicates

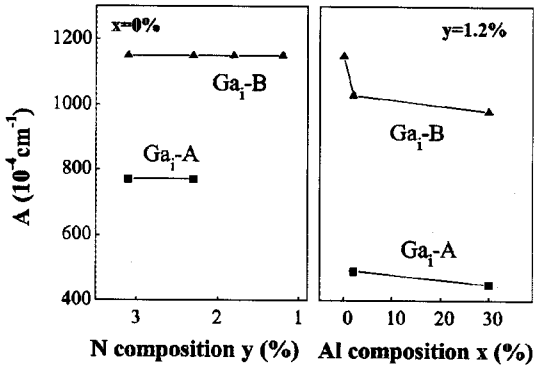

FIG. 2. The constant of hyperfine interaction with ^{69}Ga nucleus plotted as a function of Al and N compositions in $Al_xGa_{1-x}N_yP_{1-y}$. No reliable data for Ga-*A* from $GaN_{0.012}P_{0.988}$ and $GaN_{0.018}P_{0.982}$ could be obtained, as the corresponding ODMR signal was obscured by the much stronger ODMR signals from other defects that overlap within the same field range.

that Al might be present near the Ga_i-*A* and Ga_i-*B* defects, affecting the HF strength at the Ga_i. The nonlinear dependence of the HF interaction on the Al composition also indicates that the presence of Al near the defects may not necessarily be random. In other words, Al might play a role in the formation of the defects. This suggestion is supported by the fact that the ODMR intensity increases significantly upon incorporation of Al in the alloy. Note that incorporation of Al in GaAs was also required to introduce the Ga_i defects in $Al_xGa_{1-x}As$ (Refs. 9 and 10). Moreover, the strength of the HF interaction observed in $Al_xGa_{1-x}As$ alloys[9–12] is very similar to that of Ga_i-*A* in $Al_xGa_{1-x}N_yP_{1-y}$ studied here. If the defect observed in $Al_xGa_{1-x}As$ systems is indeed Ga_i-*A*, this would be an indication that the Ga_i is surrounded by group-III atoms since it is not sensitive to the variation of group-V atoms.

While the HF interaction strength of both Ga_i-*A* and Ga_i-*B* varies with Al composition, they are insensitive to N composition (Fig. 2, left panel). However, the small composition of N is essential for the formation of the Ga_i-*A* and Ga_i-*B* defects. This indicates that either N is directly involved as part of the defect or the nonequilibrium growth conditions for the incorporation of N facilitate the defect formation but without directly involving N. It is interesting to note that the HF parameter of Ga_i-*A* in GaNP, $A(^{69}Ga) = 770 \times 10^{-4}$ cm^{-1}, is very close to 741×10^{-4} cm^{-1} for Ga_i in its parent GaP.[6] The same applies to Ga_i-*A* in $Al_xGa_{1-x}N_yP_{1-y}$, i.e., $A(^{69}Ga) = (450-490) \times 10^{-4}$ cm^{-1} is very close to $\sim 500 \times 10^{-4}$ cm^{-1} for $Al_xGa_{1-x}As$ alloys.[9–12] This is an indication that N might not directly involve in Ga_i-*A*. Ga_i-*B* was never observed in N-free GaP and $Al_xGa_{1-x}As$ alloys, on the other hand. This indicates that N or the process to incorporate N could lead to the formation of the Ga_i-*B* defect.

In summary, two different Ga_i defects, i.e., Ga_i-*A* and Ga_i-*B*, are identified by ODMR for GaN_yP_{1-y} and $Al_xGa_{1-x}N_yP_{1-y}$. Both defects exhibit the characteristic HF structure arising from a strong interaction between an unpaired electron spin and the nuclear spin of Ga_i with the

fingerprint of the two naturally abundant isotopes, ^{69}Ga and ^{71}Ga. Both defects are argued to be complexes containing one Ga_i. From the compositional dependence, the likely presence of group-III atoms near the defects is suggested. Though not affecting the HF interaction, the incorporation of N is shown to play a crucial role in introducing both defects.

The financial support by the Swedish Research Council and the Wenner-Gren Foundation is greatly appreciated. The work at NREL was supported by the U.S. DOE/BES and DOE/EERE under Contract No. DE-AC36-99GO10337. The work in Thailand was supported by the Thailand Research Fund under Contract No. BRG4680003.

*Permanent address: Institute of Semiconductor Physics, Pr. Nauky 45, Kiev 03028, Ukraine.

†Electronic address: wmc@ifm.liu.se

[1] G. D. Watkins, Semicond. Semimetals **51A**, 1 (1998).

[2] B. C. Cavenett, Adv. Phys. **30**, 475 (1981).

[3] T. A. Kennedy and E. R. Glaser, Semicond. Semimetals **51A**, 93 (1998).

[4] W. M. Chen, Thin Solid Films **364**, 45 (2000).

[5] W. M. Chen, in *EPR of Free Radicals in Solids*, edited by A. Lund and M. Shiotani (Kluwer Academic, Dordrecht, 2003), p. 601.

[6] K. M. Lee, in *Defects in Electronic Materials*, edited by M. Stavola *et al.*, MRS Symposia Proceedings No. 104 (Material Research Society, Pittsburgh, 1988), p. 449.

[7] W. M. Chen and B. Monemar, Phys. Rev. B **40**, 1365 (1989).

[8] M. Godlewski and B. Monemar, Phys. Rev. B **37**, 2752 (1988).

[9] T. A. Kennedy and M. G. Spencer, Phys. Rev. Lett. **57**, 2690 (1986).

[10] T. A. Kennedy, R. Magno, and M. G. Spencer, Phys. Rev. B **37**, 6325 (1988).

[11] J. M. Trombetta, T. A. Kennedy, W. Tseng, and D. Gammon, Phys. Rev. B **43**, 2458 (1991).

[12] T. Wimbauer *et al.*, Phys. Rev. B **58**, 4892 (1998).

[13] C. Bozdog *et al.*, Phys. Rev. B **59**, 12 479 (1999).

[14] K. H. Chow, G. D. Watkins, Akira Usui, and M. Mizuta, Phys. Rev. Lett. **85**, 2761 (2000).

[15] P. N. Hai, W. M. Chen, I. A. Buyanova, B. Monemar, H. Amano, and I. Akasaki, Phys. Rev. B **62**, R10 607 (2000).

[16] P. Blaha, K. Schwarz, G. K. H. Madsen, D. Kvasnicka, and J. Luitz, WIEN2k, An Augmented Plane Wave + Local Orbitals Program for Calculating Crystal Properties (Technische Universität Wien, Vienna, Austria, 2001).

[17] F. Rong and G. D. Watkins, Phys. Rev. Lett. **58**, 1486 (1987).

[18] C. G. Van de Walle and P. E. Blöchl, Phys. Rev. B **47**, 4244 (1993).

[19] W. M. Chen and B. Monemar, Appl. Phys. A: Solids Surf. **53**, 130 (1991).

[20] In Fig. 1 the weaker intensity of the experimental ODMR lines at low fields as compared to that of the simulated ones, in the case of the *X* band ODMR spectra, can be attributed to the fact that the simulations only take into account the probabilities of magnetic-dipole-allowed electron spin resonance transitions but not the difference in recombination rates of the spin sublevels (Refs. 4 and 5), that undergo strong admixing of states at low fields due to the strong HF interaction.

[21] Calculations without relativistic effects included yield a systematically smaller A values, for, e.g., (1) Hartree-Fock calculations by Koh and Miller give $A=0.2477$ cm^{-1} or 64% of our value. (2) Our calculations without relativistic effects also give a reduced A at 65% of our present value.

[22] A. K. Koh and D. J. Miller, At. Data Nucl. Data Tables **33**, 235 (1985).

[23] J. R. Morton and K. R. Preston, J. Magn. Reson. (1969-1992) **30**, 577 (1978).

[24] G. A. Baraff and M. Schlutter, Phys. Rev. Lett. **55**, 1327 (1985).